ISSN: 2525 - 2186
Tạp chí Khoa học Lạc Hồng, **2026**, 26, 043-050

DỰ BÁO SỨC KHÁNG TRỤC CÒN LẠI CỦA KẾT CẤU ỐNG KIM LOẠI NGOÀI KHƠI BỊ ĂN MÒN

Lê Trần Minh Đạt*
Trường Đại học Công thương TP. HCM, 140 Lê Trọng Tấn, Phường Tây Thạnh, Thành phố Hồ Chí Minh
* Tác giả liên hệ: datltm@huit.edu.vn

THÔNG TIN BÀI BÁO

Ngày nhận:	06/03/2026
Ngày hoàn thiện:	19/03/2026
Ngày chấp nhận:	23/03/2026
Ngày đăng:	15/04/2026

TỪ KHÓA

Kết cấu kim loại ngoài khơi;
sự xuống cấp do ăn mòn;
Sức kháng trục;
Học máy;
Dữ liệu kiểm tra thực địa.

TÓM TẮT

Các cấu kiện ống kim loại ngoài khơi liên tục tiếp xúc với môi trường biển khắc nghiệt, nơi sự ăn mòn ảnh hưởng đáng kể đến tính toàn vẹn của kết cấu. Do đó, việc đánh giá chính xác sức kháng trục còn lại của các cấu kiện kim loại bị ăn mòn là rất cần thiết. Nghiên cứu này đề xuất một khung phân tích dựa trên dữ liệu để phân tích mối quan hệ giữa các tham số ăn mòn thu được từ quá trình kiểm tra bằng phép đo siêu âm độ dày (UTG) và khả năng kháng trục của các cấu kiện. Các đặc trưng hình học liên quan đến ăn mòn được trích xuất từ dữ liệu thực địa được sử dụng làm biến đầu vào cho một số mô hình học máy, bao gồm: Hồi quy tuyến tính, Rừng ngẫu nhiên, Support Vector Regression và XGBoost. Biến đầu ra là sức kháng trục được tính toán dựa trên các đặc tính hình học đo được. Kết quả cho thấy hiệu suất dự đoán mạnh mẽ trên các mô hình ($R^2 > 0{,}99$) và xác nhận rằng độ dày hiệu dụng và các thông số hình học chi phối khả năng chịu lực còn lại. Nghiên cứu này chứng minh tiềm năng của học máy như một công cụ bổ sung để diễn giải dữ liệu kiểm tra thực địa trong đánh giá tính toàn vẹn các kết cấu kim loại ngoài khơi.

PREDICTING RESIDUAL AXIAL RESISTANCE OF CORRODED STEEL OFFSHORE TUBULAR MEMBERS

Le Tran Minh Dat*
Ho Chi Minh City University of Industry and Trade, 140 Le Trong Tan Street, Tay Thanh Ward, Ho Chi Minh City
*Corresponding Author: datltm@huit.edu.vn

ARTICLE INFO

Received:	Mar 6th, 2026
Revised:	Mar 19th, 2026
Accepted:	Mar 23rd, 2026
Published:	Apr 15th, 2026

KEYWORDS

Steel offshore structure;
Corrosion degradation;
Axial resistance;
Machine learning;
Inspection data.

ABSTRACT

Offshore jacket tubular members are continuously exposed to harsh marine environments, where corrosion significantly affects structural integrity. Therefore, accurate assessment of the residual axial remaining resistance of corroded steel members is crucial. This study proposes a data-driven analytical framework to examine the relationship between corrosion parameters obtained from ultrasonic thickness gauge (UTG) inspections and the residual axial resistance of offshore tubular members. Corrosion-related geometric descriptors extracted from inspection data are used as input features for several machine learning models, including Linear Regression, Random Forest, Support Vector Regression, and XGBoost. The output variable is the calculated axial resistance based on the measured geometric properties. The results demonstrate strong predictive performance across the models ($R^2 > 0.99$) and confirm that effective thickness and geometric parameters dominate the residual load-carrying capacity. This study highlights the potential of machine learning as a complementary tool for interpreting field inspection data in the structural integrity assessment of steel offshore structures.

Doi: https://doi.org/10.61591/jslhu.26.1089
Available online at: https://lhj.vn

1. NTRODUCTION

The structural integrity of offshore jacket platforms is significantly compromised by marine corrosion, a complex degradation process that reduces the load-bearing capacity and operational lifespan of steel components. Traditionally, the impact of corrosion on the mechanical performance of steel has been extensively studied through surface morphology analysis and tensile tests [6, 20]. To quantify this degradation over time, various mathematical models have been proposed. One of the most foundational frameworks was developed by Komp [5], who introduced a comprehensive corrosion rating system for atmospheric and marine environments. This model, along with subsequent adaptations, has been widely utilized to evaluate the reduction in bearing capacity, reliability, and longevity of steel structures across various sectors, including marine vessels and hydraulic works [15, 16].

Recent experimental and numerical investigations have further quantified the effects of non-uniform corrosion on specific structural elements. Studies have examined the residual strength of corroded steel plates [6], the ultimate capacity of stiffened plate structures [11, 14], and the shear performance of corrugated steel plates subjected to random corrosion damage [12]. Research has also highlighted that pitting corrosion—characterized by localized metal loss—significantly affects the ultimate strength of plates under in-plane compression and bending more severely than uniform thinning [13, 20]. While these studies provide valuable insights into specific degradation scenarios, there is a clear need to cover a broader range of structural dimensions and real-world properties, particularly for offshore tubular members [21].

The assessment of residual axial resistance N_{rd} of corroded tubular members is conventionally governed by international standards such as ISO 19902 [3] and DNV-ST-F101 [2]. While these codes provide a robust foundation for design, they possess inherent limitations when applied to the reassessment of aging structures:

Deterministic nature: Traditional formulations are primarily deterministic and based on "snapshot" evaluations. They often rely on a simplified "effective thickness", which is calculated by subtracting a uniform corrosion allowance from the nominal thickness [1, 3].

Simplification of localized corrosion: In reality, marine corrosion is rarely uniform. Localized thinning, pitting, and irregular degradation patterns significantly influence the buckling behavior and ultimate capacity of tubular members [10]. Standard codes often struggle to account for the stochastic nature of these localized features without resorting to overly conservative safety factors.

Computational bottlenecks: While finite element analysis (FEA) can model complex corrosion geometries accurately [24], the computational cost is prohibitive for large-scale jackets containing thousands of members, making it impractical for rapid or real-time structural health monitoring.

In practical offshore asset management, integrity evaluations are often based on a simplified averaging approach. Asset managers typically determine the remaining design resistance by calculating the average remaining thickness over the entire member length or by assessing the percentage of metal loss against nominal design thresholds [1, 2]. This "averaging effect" creates a dangerous paradox: a member may satisfy the average thickness criteria while harboring severe localized thinning that acts as a precursor to premature failure—a gap that necessitates more granular assessment tools [11, 24].

To address these challenges, machine learning (ML) and data-driven techniques have emerged as powerful alternatives. Algorithms such as Random Forest [17] and XGBoost [4, 18] have demonstrated superior performance in capturing highly non-linear relationships within complex engineering datasets [22]. In the marine domain, ML has been deployed to predict the fatigue life of foundations [7] and estimate the remaining resistance of column components using hybrid models like GA-ANN [24]. Furthermore, the integration of Explainable AI (XAI), specifically the SHAP framework [8, 19], has enabled researchers to move beyond "black-box" predictions by providing physical interpretability to model outputs [11, 23].

This paper addresses these gaps by proposing a data-driven analytical framework using the XGBoost algorithm to investigate the relationship between corrosion-induced geometric parameters and the residual axial resistance derived from design code formulations. The main contributions of this study are summarized as follows:

Data-driven surrogate analysis of code-based resistance: A machine learning framework is developed using field ultrasonic thickness (UTG) inspection data to approximate the mapping between corrosion-related geometric indicators and the residual axial resistance calculated according to the ISO 19902 formulation. The model is used as a surrogate analytical tool to explore patterns within inspection data rather than to replace the design equation.

Beyond conventional indicators such as mean thickness, the study introduces additional corrosion descriptors derived from inspection measurements, including minimum thickness t_{min} and thickness standard deviation σ_t. These features allow the model to capture the influence of localized corrosion and non-uniform wall loss on the calculated structural resistance.

To improve interpretability, SHAP (SHapley Additive exPlanations) analysis is applied to the trained model. This approach provides quantitative insights into how different corrosion indicators and geometric variables contribute to variations in the calculated residual axial resistance, thereby supporting engineering interpretation of inspection data.

2. DATA ACQUISITION AND PRE-PROCESSING

2.1. Field data source and structural specifications

The dataset utilized in this study is derived from comprehensive underwater inspection campaigns of fixed steel offshore jacket platforms operating in tropical marine environments. The primary focus is on the primary structural members - specifically, horizontal and diagonal braces, which are most susceptible to varying degrees of corrosion.

The reference structural components consist of high-strength structural steel tubular members with the following nominal specifications: The main legs - concrete-filled steel tubes (Ø812.8 × 20.6 mm) to enhance axial stiffness. The braces - hollow circular sections Ø 530 ×12.0 mm for horizontal and diagonal framing. Material grade is S355 (specified minimum yield strength f_y = 355 MPa).

Inspection method: in-service wall thicknesses were quantified using a Cygnus 1 Heavy Duty ultrasonic thickness gauge (UTG) equipped with a single-crystal probe (2.25 MHz, 13 mm diameter).

2.2. Feature Engineering

For each tubular member, thickness measurements are obtained at discrete elevation levels with a vertical spacing of 1 m. At each elevation, four circumferential readings are recorded. Let $t_{i,j}$ denote the measured wall thickness at elevation i and direction $j (j = 1, \dots, 4)$.

The following features are derived for each member–elevation record:

Mean thickness:

$$\mu_t = \frac{1}{4}\sum_{j=1}^{4} t_{i,j} \qquad (1)$$

Minimum thickness:

$$t_{\min} = \min\,(t_{i,1}, t_{i,2}, t_{i,3}, t_{i,4}) \qquad (2)$$

Thickness variability:

$$\sigma_t = \sqrt{\frac{1}{3}\sum_{j=1}^{4} (t_{i,j} - \mu_t)^2}; \qquad (3)$$

$$\mathrm{CoV}_t = \frac{\sigma_t}{\mu_t} \qquad (4)$$

These descriptors characterize both corrosion severity and circumferential non-uniformity.

Corrosion severity indicators: based on the nominal wall thickness t_0, corrosion loss metrics are defined as:

$$\Delta t_{\text{mean}} = t_0 - \mu_t; \qquad \Delta t_{\max} = t_0 - t_{\min} \qquad (5)$$

These indicators quantify the extent of material degradation relative to the as-designed condition.

ML-ready dataset: The dataset consists of 507 inspection records obtained from offshore tubular members. Each record corresponds to a member–elevation measurement location and includes geometric parameters, corrosion indicators, and the calculated residual axial resistance. Each dataset record corresponds to a unique member–elevation combination and includes geometric properties (d, t_0), material strength (f_y), corrosion severity and variability descriptors ($\Delta t_{\text{mean}}, \Delta t_{\max}, t_{\min}, \sigma_t, \mathrm{CoV}_t, \mu_t$), and elevation (z). The output variable is the axial design resistance N_{Rd}, calculated according to ISO 19902 using inspection-informed section properties:

$$N_{\text{rd}} = \frac{A_{eff} f_y}{\gamma_M} \qquad (6)$$

where f_y is the yield strength, A_{eff} is the cross-sectional area, and $\gamma_M = 1.08$ is the partial resistance factor [2].

The input and output variables ar presented in table 1

Table 1. *Statistical indicators of the input and output variables*

Variable	Description	Unit	Min	Max	Mean	Std. dev.
D	Outer diameter of tubular member	mm	530	812.8	703.82	137.8
t_0	Nominal wall thickness	mm	12	20.6	17.29	4.19
f_y	Steel yield strength	MPa	355	355	355	0
Δt_{mean}	Mean wall thickness loss	mm	-1.6	6.5	2.22	1.45
$\Delta t_{\max}$	Maximum wall thickness loss	mm	-1.4	9.8	3.57	1.92
$t_{\min}$	Minimum measured wall thickness	mm	3.9	22	13.72	4.29
σ_t	Standard deviation of thickness measurements	mm	0	3.57	1.19	0.73

Variable	Description	Unit	Min	Max	Mean	Std. dev.
CoV_t	Coefficient of variation of thickness	–	0	0.4	0.086	0.063
μ_t	Mean measured wall thickness	mm	6	22.2	15.07	4.30
z	Height above mean sea level	m	0	15	7.58	4.56
N_{rd}	Axial resistance (output)	MN	2117.70	17956.60	10296.57	4581.45

The statistical indicators reveal substantial variability in corrosion severity and thickness distribution, particularly at lower elevations, highlighting the necessity of incorporating both corrosion magnitude and variability metrics into the machine learning framework (fig. 1).

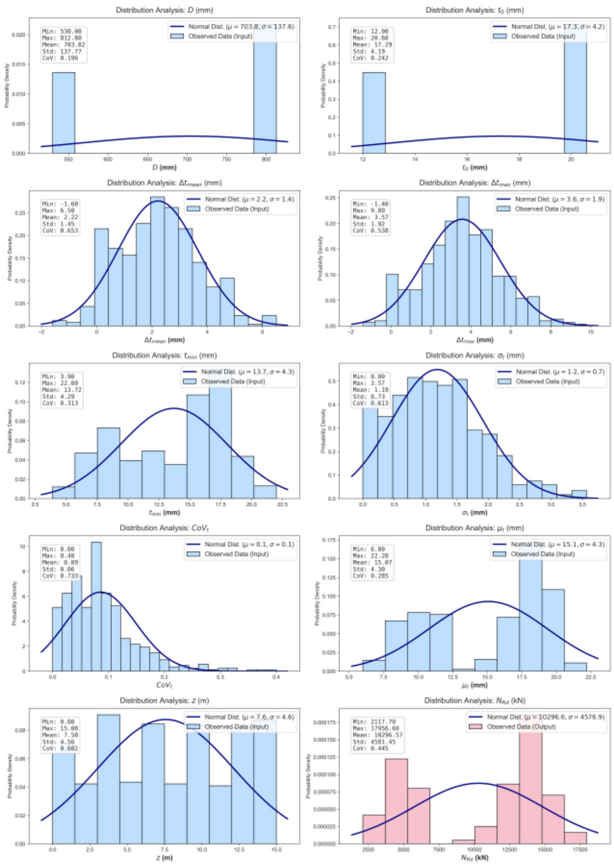

Figure 1. *Histogram of input and output parameters.*

The correlation maxtrix of input and output parameters are showed in fig. 2.

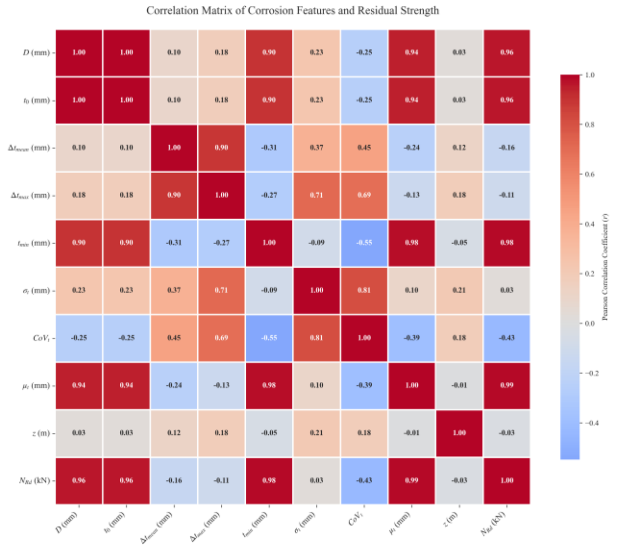

Fig. 2. *Pearson correlation coefficients of input and output parameters.*

2.3. Data pre-processing

A robust pre-processing pipeline was executed to ensure data integrity and model reliability. First, to address inspection heterogeneity, the varying density of measurement grids was standardized into consistent statistical moments (mean, minimum, and standard deviation) for each structural member. Subsequently, feature scaling was applied using StandardScaler to normalize variables of different units (e.g., elevation in meters vs. thickness in millimeters), preventing bias during gradient-based optimization.

3. METHOLOGY

3.1. Theoretical background: ISO 19902 and DNV-ST-F101

The foundation of this study is based on the limit state design principles established in ISO 19902 and DNV-ST-F101. For offshore tubular members subjected to axial loads, the design tensile resistance N_{rd} is conventionally calculated by equation (5).

However, this study argues that such deterministic approaches fail to account for the stress concentration and localized instability caused by non-uniform thinning. Our methodology moves beyond these simplified formulations by using a data-driven approach that learns the complex relationship between various statistical corrosion features and the actual structural capacity.

3.2. Machine learning algorithms and benchmarking

The feature vector x integrates input variables:

$$x = \{d, t_0, f_y, \Delta t_{mean}, \Delta t_{max}, t_{min}, \sigma_t, CoV_t, \mu_t, z\} \qquad (7)$$

To identify the most robust surrogate model, a benchmarking process was conducted among four distinct classes of algorithms:

• Linear Regression (LR): Serves as the baseline model, assuming a linear combination of features:

$$\hat{y} = \beta_0 + \sum_{j=1}^{p} \beta_j x_j \tag{8}$$

• Support Vector Regression (SVR): Unlike models that minimize the sum of squared residuals, SVR seeks a function $f(x)$ that possesses at most ε deviation from the actual targets for all training data. The optimization problem is formulated to find the flattest tube that contains the data points:

$$min\ \frac{1}{2}\ ||w||^2 +\ C\sum_{i=1}^{n}(\xi_i + \xi_i^*) \tag{9}$$

Subject to the constraints:

$$\begin{cases} y_i - \langle w, \phi(x)\rangle - b \le \epsilon + \xi_i \\ \langle w, \phi(x)\rangle + b - y_i \le \epsilon + \xi_i^* \\ \xi_i, \xi_i^* \ge 0 \end{cases} \tag{10}$$

• Random Forest (RF): An ensemble bagging technique that reduces variance by averaging multiple decision trees.

$$\hat{y} = \frac{1}{T}\sum_{T=1}^{T} f_t(x) \tag{11}$$

RF reduces variance through bagging and random feature selection.

• Extreme Gradient Boosting (XGBoost): The objective function of XGBoost at iteration t is defined as:

$$Obj^t = \sum_{i=1}^{n} L\left(y_i, \hat{y}_i^{(t-1)} + f_t(x_i)\right) + \Omega(f_t) \tag{12}$$

3.3. Model training and hyperparameter optimization

Training and lalidation strategy: to evaluate the models' predictive capability on unseen data, the dataset was partitioned into an 80% training set and a 20% testing set. A 5-fold cross-validation scheme was integrated during the training phase. This approach ensures that the performance metrics are statistically robust and independent of any specific data split, effectively mitigating potential bias from the stochastic nature of corrosion patterns.

Hyperparameter tuning: a systematic Grid search was employed to optimize the architectural parameters of the XGBoost and SVR models. For XGBoost, critical hyperparameters—including the learning rate (η), maximum tree depth (max $\_depth$), and subsample ratio—were fine-tuned to balance model complexity with generalization. This optimization allows the model to capture the highly non-linear degradation trends inherent in marine jacket structures without over-sensitizing to local noise in the ultrasonic thickness gauge (UTG) measurements.

3.4. Model interpretability framework (SHAP)

To bridge the gap between "black-box" machine learning and physical engineering intuition, we employed SHapley Additive exPlanations (SHAP). Based on cooperative game theory, SHAP assigns an importance value to each feature for every prediction:

$$g(z') = \phi_0 + \sum_{j=1}^{M} \phi_j z_j' \tag{13}$$

3.5. Performance evaluation metrics

The accuracy of the predictive models was evaluated using three standard statistical metrics:

Coefficient of Determination (R^2): Measures the proportion of variance explained by the model:

$$R^2 = 1 - \frac{(y_i - \hat{y}_i)^2}{(y_i - \bar{y})^2} \tag{14}$$

Root Mean Square Error (RMSE): Provides a measure of the average magnitude of the error, penalizing larger deviations.

$$RMSE = \sqrt{\frac{1}{n}\sum (y_i - \hat{y}_i)^2} \tag{15}$$

Mean Absolute Error (MAE): Represents the average absolute difference between predicted and actual resistance values.

$$MAE = \frac{1}{n}\sum_{i=1}^{n} |y_i - \hat{y}_i| \tag{16}$$

4. RESULTS AND DISCUSSION

4.1. Model performance and benchmarking

The evaluated machine learning models demonstrate very high predictive accuracy, with the XGBoost model achieving the best performance ($R^2 > 0.99$). This high accuracy is expected because the target variable N_{rd} is calculated using the ISO 19902 design formulation, which establishes a largely deterministic relationship between structural capacity and the geometric parameters used as input features.

In this context, the machine learning models do not replace the design equation but rather act as surrogate approximators of the relationship between corrosion-derived thickness features and the calculated axial resistance. The results indicate that ensemble-based models, particularly XGBoost, are effective in capturing the nonlinear interactions among thickness statistics and geometric variables. The predictive accuracy of the proposed XGBoost framework was evaluated against other models using the dataset. The statistical properties of N_{rd} using ML models on training and testing set show in table 2.

Table 2. *Statistical properties of N_{rd} using ML models on training and testing set*

Model	Training set			Testing set		
	R^2	RMSE (kN)	MAE (kN)	R^2	RMSE (kN)	MAE (kN)
MLR	0.9985	172.82	131.90	0.9984	185.34	147.91
SVR	0.9077	1381.59	1113.92	0.8958	1483.01	1203.62
RF	0.9992	84.39	24.83	0.9991	84.51	27.10
XGBoost	0.9998	58.54	14.55	0.9999	46.00	18.47

Specifically, the XGBoost model achieved a coefficient of determination R^2 exceeding 0.99, with a remarkably low Root Mean Square Error (RMSE). his high level of accuracy can be explained by the deterministic nature of the target variable used in the study.

4.2. Residual analysis and error distribution

To further validate the reliability of the models, a residual plot (Fig. 4) between MLR and XGB was analyzed. This plot illustrates the difference between the predicted and actual resistance values.

The MLR residuals exhibited a clear systematic pattern (bias), particularly at the higher and lower ends of the resistance spectrum, suggesting a "lack of fit" for non-linear degradation.

The XGBoost residual shows a stochastic distribution concentrated heavily around the zero-error baseline.

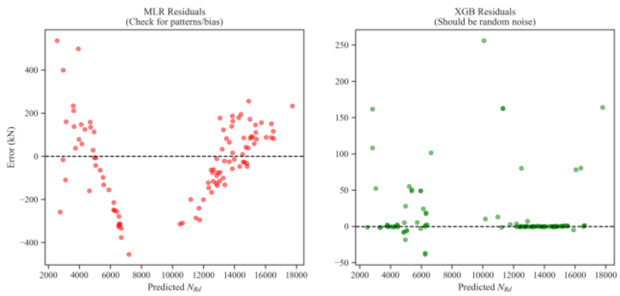

Figure 4. *Residual predicted model MLR vs XGBoost*

This homoscedastic behavior confirms that XGBoost is an unbiased estimator. For offshore engineering applications, this lack of bias is crucial, as it ensures that the safety margins are not systematically underestimated in high-risk zones, such as the splash zone.

4.3. Feature importance analysis (Gini importance)

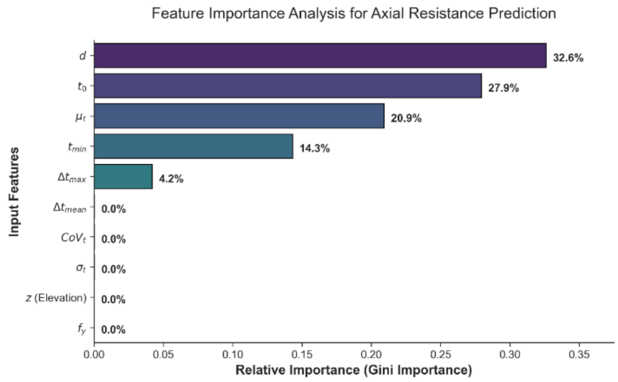

Figure 5. *Feature importance analysis of input parameters*

The relative importance of input features was evaluated using Gini Importance, as illustrated in Fig. 5. The results indicate that the structural geometry, specifically the diameter d and initial thickness t_0, remains the primary determinant of axial resistance, contributing 32.6% and 27.9%, respectively. Furthermore, the model demonstrates a high sensitivity to corrosion-induced degradation, with the mean residual thickness μ_t and minimum thickness t_{min} accounting for a combined 35.2% of the importance. Notably, the significance of t_{min} highlights the model's ability to account for localized structural vulnerability. Conversely, secondary statistical metrics such as CoV_t and σ_t showed negligible influence, suggesting that the core geometric and extreme corrosion parameters provide sufficient information for high-fidelity strength prediction.

4.4. Global interpretability using SHAP values

To bridge the gap between "black-box" machine learning and structural mechanics, a SHAP analysis was conducted on the optimized XGBoost model. Fig. 6 illustrates the distribution of SHAP values, representing the contribution of each feature to the final axial resistance prediction N_{rd}.

The global geometry parameters, diameter d and initial thickness t_0, exhibit the most significant impact on the model output.

Positive Correlation: High feature values (red dots) for d and t_0 are strictly associated with high positive SHAP values. This aligns with the fundamental structural formula N_{rd} in eq. (5), where an increase in cross-sectional area directly enhances load-bearing capacity.

Impact Magnitude: d shows the widest horizontal spread (from -2000 to +1500), indicating it is the most influential factor in differentiating strength across the dataset.

The SHAP analysis provides critical insights into how the model perceives corrosion damage:

Critical vulnerability t_{min}: the variable t_{min} shows a wide distribution of SHAP values. High values of t_{min}

(red) correspond to positive SHAP values, while low values (blue) significantly reduce the predicted N_{rd}. The long "tail" of blue dots extending to the left suggests that severe localized pitting (very low t_{min}) can lead to a drastic, non-linear drop in structural integrity.

Mean residual thickness μ_t: similar to t_0, μ_t follows a clear positive trend. However, its tighter clustering indicates a more stable and predictable influence on strength compared to the localized volatility of t_{min}.

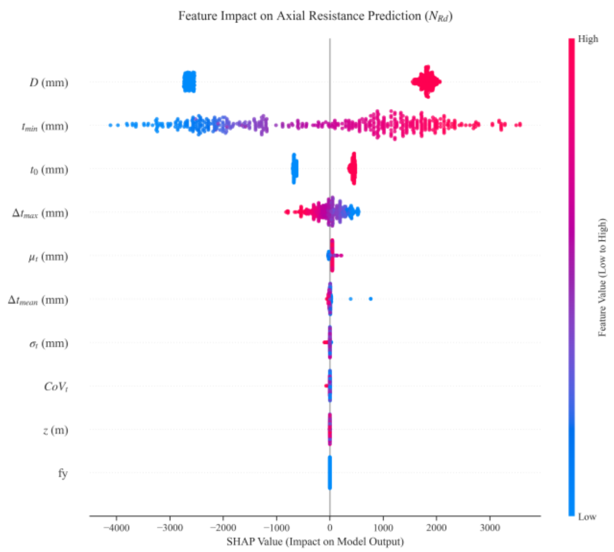

Figure 6. *SHAP analysis for input parameters*

Negative impact of max loss Δt_{max}: inversely, high values of Δt_{max} (red dots) are positioned on the left side of the axis (negative SHAP values). This confirms that the model correctly identifies maximum thickness loss as a primary degradation factor that penalizes the axial strength.

Redundant features: features such as z (elevation), f_y and CoV_t show SHAP values concentrated at zero. This confirms that for this specific dataset and jacket structure, these variables provide negligible marginal information, justifying their zero-importance rating in the previous Gini analysis.

The application of explainable AI techniques provides additional engineering insights by quantifying the relative importance of corrosion indicators such as minimum thickness and thickness variability. These results highlight how data-driven models can assist engineers in interpreting large inspection datasets and identifying the corrosion characteristics that most strongly influence the calculated structural resistance.

4.5. Engineering discussion

The predictive framework developed in this study, particularly the XGBoost model, should be interpreted as a data-driven surrogate of the ISO 19902 design formulation rather than a replacement for it. The high predictive performance (R^2 > 0.99) reflects the underlying deterministic relationship between geometric properties and axial resistance defined by the design code. Accordingly, the machine learning models primarily approximate this mapping, enabling rapid evaluation of structural capacity without explicitly reapplying the full analytical formulation.

The practical advantage of this approach becomes evident in scenarios involving large-scale inspection datasets, where thousands of UTG measurements must be processed and interpreted. In such cases, the surrogate model significantly reduces computational effort and enables near real-time assessment within digital inspection workflows. In addition, the framework provides flexibility in handling incomplete or noisy inspection data, where direct application of design equations may be less straightforward.

From an engineering interpretation perspective, SHAP analysis confirms that the model is highly sensitive to minimum thickness t_{min} and maximum thickness loss Δt_{max}, consistent with the "weakest-link" behavior of corroded members. This allows the framework not only to approximate the calculated resistance but also to highlight critical corrosion features that govern capacity reduction. Overall, the proposed approach serves as a practical tool for supporting engineers in the interpretation and prioritization of inspection data, rather than replacing established design methodologies.

5. CONCLUSION

This study presented a data-driven framework for analyzing the influence of corrosion features on the residual axial resistance of offshore tubular members using field UTG inspection data. The main findings are summarized as follows:

• Among the evaluated models, XGBoost provided the highest predictive accuracy, demonstrating strong capability in learning nonlinear relationships between corrosion indicators and calculated structural resistance.

• The analysis confirms that minimum remaining thickness is the most influential corrosion parameter affecting axial resistance.

• Although elevation (z) shows low importance in SHAP analysis, it remains a useful environmental proxy. It indirectly reflects corrosion exposure conditions, particularly in the splash zone, where degradation variability is more pronounced.

Overall, the proposed approach provides a practical surrogate modeling tool that can assist engineers in rapidly interpreting inspection data and identifying potential structural risks.

Future research will focus on integrating probabilistic corrosion growth models and incorporating nonlinear structural simulations to further improve predictive capability and support long-term integrity management.

6. REFERENCES

[1] American Petroleum Institute, Recommended practice for planning, designing and constructing fixed offshore platforms—Working stress design (API RP 2A-WSD), American Petroleum Institute, 2014.

[2] DNV AS, Submarine pipeline systems (DNV-ST-F101), DNV AS, 2021.

[3] International Organization for Standardization, Petroleum and natural gas industries — Fixed steel offshore structures (ISO 19902), 2007.

[4] T. Chen, C. Guestrin, XGBoost: A scalable tree boosting system, Proc. 22nd ACM SIGKDD Int. Conf. Knowl. Discov. Data Min., 2016, 785–794.

[5] M. Komp, Atmospheric corrosion ratings of weathering steels—Calculation and significance, Mater. Perform., 1987, 26 (7), 42–44.

[6] Y. Wang, S. Xu, H. Wang, A. Li, Predicting the residual strength and deformability of corroded steel plate based on the corrosion morphology, Constr. Build. Mater., 2017, 152, 777–793.

[7] X. Liu et al., Physics-informed machine learning for corrosion fatigue life prediction of offshore wind turbine foundations, Reliab. Eng. Syst. Saf., 2022, 218, 108151.

[8] S. M. Lundberg, S. I. Lee, A unified approach to interpreting model predictions, Adv. Neural Inf. Process. Syst., 2017, 30.

[9] R. E. Melchers, Corrosion uncertainty modeling for offshore structures, J. Constr. Steel Res., 1999, 52 (1), 3–19.

[10] J. K. Paik, Ultimate limit state analysis and design of steel structures, John Wiley & Sons, 2018.

[11] Y. Zhu, C. Guedes Soares, Data-driven models for the ultimate strength of corroded stiffened plates, Mar. Struct., 2023, 88, 103345.

[12] Z. Zhao, J. Liu, B. Zhao, Z. Jin, X. Jian, N. Zhang, Shear capacity of corrugated steel plates with a random corrosion damage, Thin-Walled Struct., 2023, 193, 111264.

[13] T. Nakai, H. Matsushita, N. Yamamoto, Effect of pitting corrosion on the ultimate strength of steel plates subjected to in-plane compression and bending, J. Mar. Sci. Technol., 2006, 11, 52–64.

[14] Y. Wang, J. A. Wharton, R. A. Shenoi, Ultimate strength assessment of steel stiffened plate structures with grooving corrosion damage, Eng. Struct., 2015, 94, 29–42.

[15] D.-D. Nguyen, T.-H. Nguyen, Reliability evaluation of 2D semi-rigid steel frames accounting for corrosion effects, J. Mater. Eng. Struct., 2022, 9 (3), 339–353.

[16] S.-M. Nguyen, V.-L. Phan, N.-L. Tran, X.-H. Nguyen, T.-H. Nguyen, Time-dependent reliability assessment of a continuous I-shaped steel beam considering corrosion effects, Eng. Technol. Appl. Sci. Res., 2022, 12 (6), 9523–9526.

[17] L. Breiman, Random forests, Mach. Learn., 2001, 45 (1), 5–32.

[18] T. Chen, C. Guestrin, XGBoost: A scalable tree boosting system, Proc. 22nd ACM SIGKDD Int. Conf. Knowl. Discov. Data Min., 2016.

[19] S. M. Lundberg, S. I. Lee, A unified approach to interpreting model predictions, Adv. Neural Inf. Process. Syst. (NIPS), 2017.

[20] S. H. Xu, C. Guedes Soares, Uncertainty in the ultimate strength of steel plates with pitting corrosion, Struct. Saf., 2012, 34 (1), 211–218.

[21] H. Ahmadi, M. A. Lotfollahi-Yaghin, Stress concentration factors of central brace in statically loaded multi-planar tubular XT-joints, Ocean Eng., 2012, 47, 130–148.

[22] S. Mangalathu, J. S. Jeon, Classification of failure modes of RC bridge columns using machine learning techniques, Eng. Struct., 2018, 160, 226–234.

[23] Y. Zhu, C. Guedes Soares, Reliability analysis of stiffened panels with pitting corrosion using machine learning, Mar. Struct., 2022, 82, 103137.

[24] D.-D. Nguyen, N.-G. Tran, V.-C. Ho, Tr.-H. Nguyen, Prediction of remaining design resistance and bending stiffness of the steel column base plate considering metal corrosion using GA-ANN model, Case Stud. Constr. Mater., 2024, 21, e03930.